Materials Science and Engineering B 191 (2015) 33–40

Contents lists available at ScienceDirect

Materials Science and Engineering B

journal homepage: www.elsevier.com/locate/mseb

Synthesis and thermal stability of two-dimensional carbide MXene Ti_3C_2

Zhengyang Li, Libo Wang, Dandan Sun, Yude Zhang, Baozhong Liu, Qianku Hu, Aiguo Zhou *

Cultivating Base for Key Laboratory of Environment-friendly Inorganic Materials in University of Henan Province, School of Materials Science and Engineering, Henan Polytechnic University, Jiaozuo, Henan 454000, China

ARTICLE INFO

Article history:
Received 10 May 2014
Received in revised form 11 October 2014
Accepted 22 October 2014
Available online 3 November 2014

Keywords:
Two-dimensional materials
MXene
Transition metal carbides
Thermal stability
Exfoliation

ABSTRACT

We investigated the synthesis of quasi-two-dimensional carbide (Ti_3C_2), with the name of MXene, by immersing Ti_3AlC_2 in 40% or 49% hydrofluoric acid (HF) at 0 °C, 15 °C or 60 °C. The influences of time, temperature, and source of Ti_3AlC_2 on the synthesis were researched. It was found that Ti_3C_2 synthesized from pressureless synthesized Ti_3AlC_2 was highly oriented compared to that from hot-pressed Ti_3AlC_2. As-synthesized Ti_3C_2 could be further exfoliated by intercalation with urea, dimethylsulfoxide or ammonia. From the results of thermogravimetry and differential scanning calorimetry, Ti_3C_2 MXene with F/OH termination was found to be stable in argon atmosphere at temperature up to 800 °C. In oxygen atmosphere, at 200 °C, parts of MXene layers were oxidized to obtain an interesting structure: anatase nano-crystals were evenly distributed on 2D Ti_3C_2 layers. At 1000 °C, MXene layers were completely oxidized and anatase phase fully transformed to rutile in oxygen atmosphere.

1. Introduction

Two-dimensional (2D) materials, such as graphene [1], are well known to have unique properties and important applications. In general, 2D materials are produced by exfoliating layered 3D materials with weak van der Waals-like coupling between layers. During the last decade, some 2D materials such as hexagonal boron nitride [2], metal oxides [3], and chalcogenides [4] have been synthesized by chemical exfoliation or mechanical cleavage of layered 3D precursors.

However, there was no report on the synthesis of 2D nanocrystalline materials by exfoliation of layered solids with strong primary bonds until Naguib et al. [5,6] synthesized two-dimensional transition metal carbides by HF exfoliating from MAX phases: Ti_3AlC_2, Ti_2AlC, etc. These 2D materials were made by removing "A" element from MAX phase and named as MXenes to emphasize their graphene-like morphology. MXenes are conductive and hydrophilic 2D materials. From experiments [7–9] and theoretic computation [10], MXenes are very promising electrode materials for lithium-ion batteries and supercapacitors. Additionally, we found that MXene are promising hydrogen storage medium [11], lead adsorption medium [12], and catalyst [13]. The research on MXenes opened a door for the synthesis of a large number of 2D $M_{n+1}X_n$ structures and attracted the attention of many scientists [14–16].

MAX phases, the precursors of MXenes, are ternary carbides or nitrides with the general formula of $M_{n+1}AX_n$, where M is an early transition metal; A is an A-group element (mostly group IIIA or IVA); X is either carbon or nitrogen and the value of n can be 1, 2, or 3 [17–20]. A typical MAX compound consists of metallic A layers and ceramic $M_{n+1}X_n$ layers. A layers are chemically more active than $M_{n+1}X_n$ layers [21]. 2D MXenes were made by removing A layers from MAX phases by HF etching [5,6]. The surfaces of MXene made in HF solution are usually terminated by F and/or OH groups due to its high surface energy. Fig. 1 shows the chemical structures of a typical MAX phase (Ti_3AlC_2) and MXene (Ti_3C_2) with OH termination. The later can be made from the former by HF etching and sonication.

Thereafter, many theoretic papers predicted the properties and applications of these novel 2D materials [10,11,16,22–25]. However, there are only a few reports on the experimental synthesis and characterization of MXenes.

In this paper, for fully understanding MXene synthesis process, Ti_3C_2 MXene was made by exfoliating Ti_3AlC_2 with HF acid at different temperature for different time. In order to further exfoliate 2D MXene, as-synthesized MXenes were intercalated with urea, dimethylsulfoxide or $NH_3{\cdot}H_2O$.

Besides the synthesis procedure, we studied the thermal stability of Ti_3C_2 2D sheets in oxygen or argon atmosphere. This property

* Corresponding author. Tel.: +86 391 3986936; fax: +86 391 3986908.
E-mail address: zhouag@hpu.edu.cn (A. Zhou).

http://dx.doi.org/10.1016/j.mseb.2014.10.009
0921-5107/

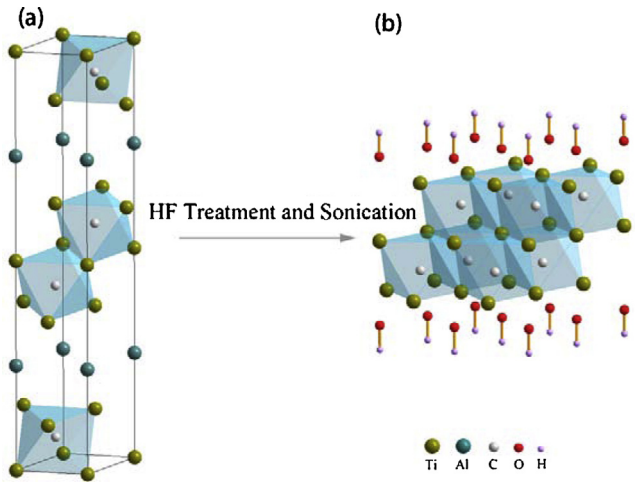

Fig. 1. Chemical structures of (a) Ti_3AlC_2 (a typical MAX phase), and (b) Ti_3C_2 (a typical MXene) with OH termination. Ti_3C_2 is made from Ti_3AlC_2 by HF etching and sonication.

is very important for the application of these materials at high temperature. As far as the authors know, this is the first report on the experimental measurement of MXenes' thermal stability. Additionally, the thermal process of MXenes in oxygen atmosphere obtained an interesting structure, that anatase nano-crystals were evenly distributed on conductive 2D Ti_3C_2 layers.

2. Experimental

Two kinds of Ti_3AlC_2 powders were used in this paper. One (HP-Ti_3AlC_2, 98 wt.% pure) was obtained by grinding hot-pressed (HP) Ti_3AlC_2, which was made from 3Ti/Al/2C mixture by hot-press at 1400 °C under 25 MPa for 2 h with a heating rate of 20 °C/min. The other (PLS-Ti_3AlC, 98 wt.% pure) was pressureless synthesized powders from TiH_2/Al/2TiC by a tube furnace with flowing Ar atmosphere at 1450 °C for 2 h with a heating rate of 15 °C/min [26]. Both HP-Ti_3AlC_2 powders and PLS-Ti_3AlC_2 powders passed through a 325-mesh screen. Ten grams of Ti_3AlC_2 were immersed in 100 ml 40% or 49% HF solutions (Aladdin Reagent, Shanghai, China). The solution was stirred for 1 min, and then kept at different temperature (0 °C, 15 °C, or 60 °C). After some time, the samples were washed by deionized water and MXene powders were centrifugally separated from supernatant. The powders were washed by deionized water until the pH value ≈ 7, then washed by ethanol twice. Thereafter, they were dried in a vacuum oven at 80 °C for 24 h.

The intercalation experiment was carried out with dimethyl sulfoxide (DMSO), urea, or $NH_3 \cdot H_2O$, respectively. The intercalation procedure was: (1) 0.5 g MXene powders were mixed with 10 ml DMSO and then magnetically stirred for 18 h at room temperature; (2) 0.5 g MXene powders were mixed with 6 ml $NH_3 \cdot H_2O$ (25–28%) and then magnetically stirred for 2 h at room temperature; (3) 0.5 g powders were mixed with 3 g urea and 10 ml water, then magnetically stirred for 24 h at 60 °C. Thereafter, the samples were washed several times by deionized water and then dried in a vacuum oven at 80 °C.

X-ray diffraction (XRD) patterns were obtained from powders directly without further treatment with a diffractometer (Brukeraxs Co., Germany) using Cu K_α radiation. A scanning electron microscopy (FESEM, S4800, Hitachi, Japan) with an accelerating voltage of 3 kV, and equipped with an energy dispersive spectrometer (EDS, EMAX ENERGY EX-250, Horiba, Japan), was used to obtain microstructure images. Transmission electron microscope (TEM, JEOL JEM-2100, Japan) with an accelerating voltage of 200 kV, was used to investigate the structure of some 2D MXene powders.

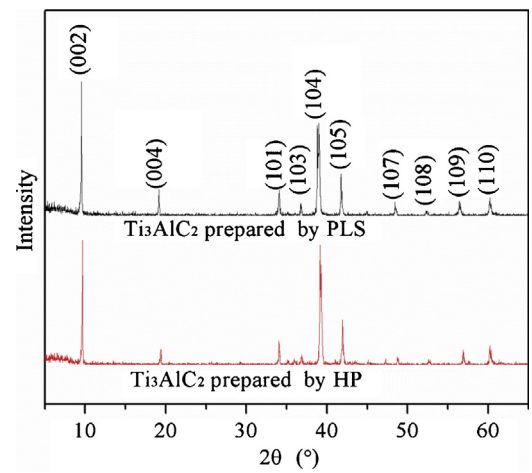

Fig. 2. XRD patterns of Ti_3AlC_2 as starting material.

Thermal stability of obtained MXene was measured by using a Setaram Evolution 2400 thermal analyzer with α-Al_2O_3 pans under argon/oxygen flow of 20 ml/min with a heating rate of 15 °C/min from room temperature (RT) to 1000 °C.

3. Results

3.1. XRD analysis of exfoliation process to synthesize MXene

The XRD patterns of two Ti_3AlC_2 powders as starting materials are shown in Fig. 2. The two patterns are very similar and both show peaks corresponding to quite pure Ti_3AlC_2. Fig. 3 shows the XRD patterns of samples exfoliated by 40% HF or 49% HF at 0 °C for 2 h, 24 h or 72 h, respectively. For either 2 h or 24 h etching, the etched samples still mainly consisted of Ti_3AlC_2 without Ti_3C_2 MXene. If etching time was extended to 72 h, the strongest peak of Ti_3AlC_2, (1 0 4) peak at 39.2°, obviously decreases. Therefore, part of Ti_3AlC_2 reacted with HF to form Ti_3C_2. In the figure, (0 0 2) peak at 9.7° and (0 0 4) peak at 19.4° are bifurcated into two minor peaks. One minor peak keeps in the original position, which belongs to Ti_3AlC_2. The other minor peak shifts to low angle, which belongs to newly formed Ti_3C_2 MXene. A conclusion can be drawn that, at 0 °C, no matter what the concentration of HF acid was, at least 72 h was required for the beginning of Ti_3AlC_2 exfoliation.

Fig. 4 shows the XRD patterns of samples processed at 15 °C. Similar with the 0 °C results shown in Fig. 3, at least 72 h was required for the exfoliation of Ti_3AlC_2. As shown in Fig. 4b, for 72 h sample, a new peak at 9.1° appeared near the (0 0 2) peak of Ti_3AlC_2 at 9.7°. The 9.1° peak belonged to Ti_3C_2 MXene. A long exfoliating time, 168 h, resulted extensive generation of MXene as shown in the figure. However, there was a little residual Ti_3AlC_2 in 40% HF sample and some TiC was formed in 49% HF sample. Therefore, at 15 °C, 168 h was not long enough to make pure MXene by 40% HF exfoliation while it was too long for the process of 49% HF exfoliation.

Theoretically, high temperature and high concentration of HF are favorable for the synthesis of MXene. Fig. 5 shows the XRD patterns of sample exfoliated at 60 °C by 49% HF. Different from literature reports [5,27], 2 h was not enough for the fully exfoliation of Ti_3AlC_2. As processing time increased, Ti_3AlC_2 peaks decrease and MXene peaks appear obviously only if the time >8 h. Weak peaks of Ti_3AlC_2 are still detectable at 12 h sample. However, for 24 h sample, all Ti_3AlC_2 was exfoliated and transformed to MXene with some TiC impurity.

To understand the influence of Ti_3AlC_2 source on the exfoliating process, MXene was made from PLS-Ti_3AlC_2 or HP-Ti_3AlC_2, by 49%

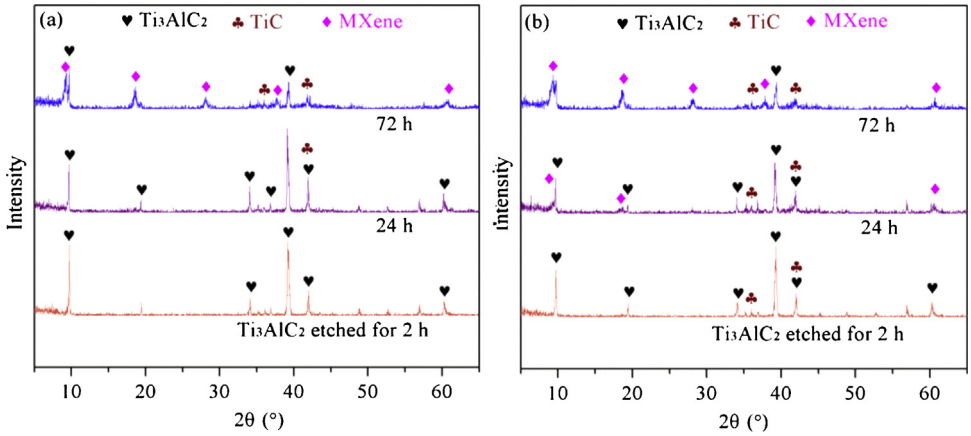

Fig. 3. XRD patterns of exfoliating Ti_3AlC_2 at 0 °C by (a) 40% HF, and (b) 49% HF.

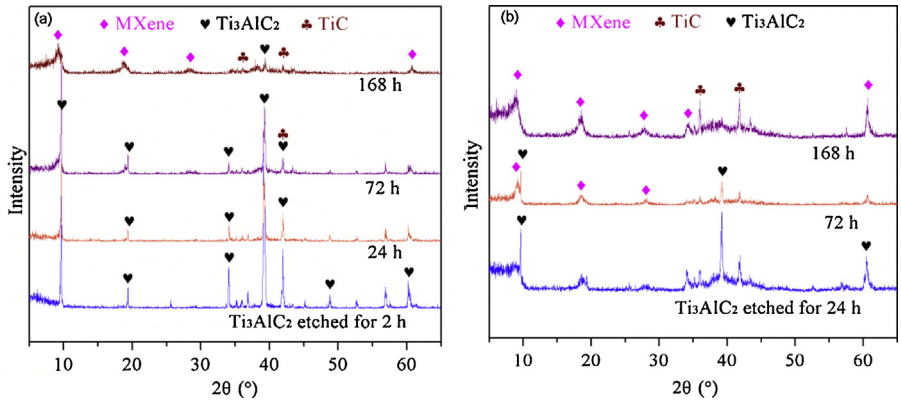

Fig. 4. XRD patterns of exfoliating Ti_3AlC_2 at 15 °C by (a) 40% HF, and (b) 49% HF.

HF etching at 60 °C for 24 h. The corresponding XRD patterns are shown in Fig. 6. MXene from PLS-Ti_3AlC_2 has stronger characteristic peaks than that from HP-Ti_3AlC_2. MXene from PLS-Ti_3AlC_2 has very strong (0 0 2) and (0 0 4) diffraction peaks as shown in Fig. 6.

Intercalation with small molecules can result in the increase of *d*-spacing of MXene and be helpful to the further exfoliation of MXene 2D sheets [28]. In this paper, the obtained MXene was intercalated with $NH_3{\cdot}H_2O$, dimethyl sulphoxide (DMSO) and urea. XRD patterns of intercalated MXene are shown in Fig. 7. For $NH_3{\cdot}H_2O$ and DMSO intercalations, the (0 0 2) peak of MXene shifts to low angle and tends to broaden, corresponding to an increase of *d*-spacing and a decline of the thickness of Ti_3C_2 layers, respectively. Therefore, the intercalation can further exfoliate MXene and is an effective way to obtain Ti_3C_2 with smaller thickness and larger *d*-spacing. However, the intercalation with urea at 60 °C for 24 h shows a very different result. The *c* lattice parameter (*LP c*) increased from 19.853 Å to 25.108 Å and, meanwhile, the (0 0 2) peak became extraordinarily strong and sharp. This means that MXene layers became thicker. During intercalation process, urea

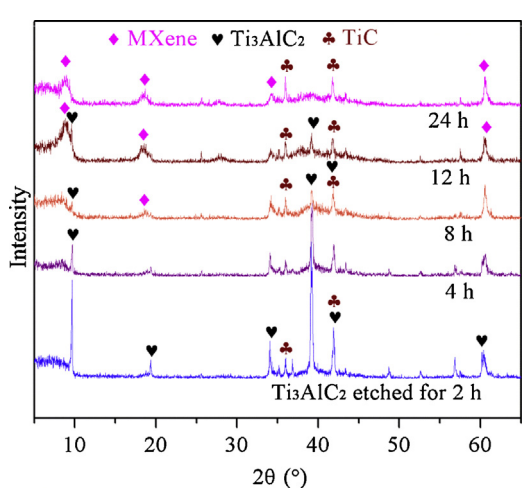

Fig. 5. XRD patterns of exfoliating Ti_3AlC_2 at 60 °C by 49% HF.

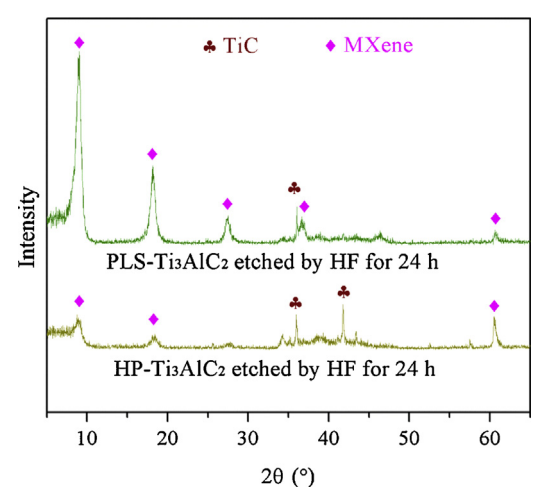

Fig. 6. XRD patterns of MXene from PLS-Ti_3AlC_2 and HP-Ti_3AlC_2 by 49% HF etching at 60 °C for 24.

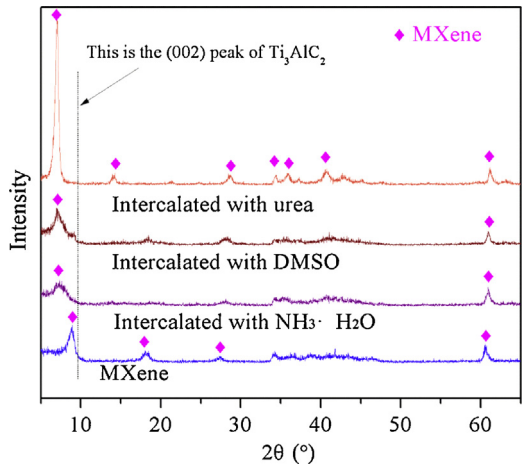

Fig. 7. XRD patterns of MXene and MXene intercalated with $NH_3 \cdot H_2O$, dimethyl sulphoxide (DMSO) and urea. The dash vertical line in 9.7° represents the original (0 0 2) peak of Ti_3AlC_2.

molecules probably came into the space between MXene crystal planes, increased *d*-spacing and *LP c* (*LP c* = *d*-spacing + thickness of 2D sheet), and meanwhile glued the MXene layers together rather than delaminated the MXene layers.

3.2. SEM and TEM analysis of MXene crystals

Fig. 8 shows the SEM images of exfoliated samples by 49% HF at 60 °C. As shown in Fig. 8a and b, only partial exfoliation appeared in Ti_3AlC_2 grains after 4 h or 8 h etching and Ti_3AlC_2 was still the main composition of etching products as shown in the XRD results.

If reaction time was extended up to 24 h, fully exfoliation was achieved and quasi-2D MXene sheets were obtained as shown in Fig. 8c and d. The whole grain exfoliated into thin layers with uniform thickness was clearly visible in high magnification SEM image (Fig. 8d) and the expansion of the grain in *c* direction is much larger than that of Fig. 8a and b in consideration of the same magnification. From high magnification image (Fig. 8e and f), the thickness of MXene layer is ~30 ± 5 nm, which corresponds to roughly 15 Ti_3C_2 layers. Additionally, Fig. 8e and f reveals two kinds of structure for the 2D layered edge. One is attached by small balls with the diameter of 40 ± 10 nm (Fig. 8e); the other is clean without any attachments (Fig. 8f). From the shape of these small balls (Fig. 8e), they were not formed by breaking larger MXene sheets or MAX particles. We conjectured that they nucleated and grew from HF solution.

From EDS, the samples in Fig. 8c contain Ti, C, F, O and Al elements with atomic ratio of Ti:C:F:O:Al = 28:20:33:18:1. It should be noted that H is not detectable to EDS. At previous literature [27], the Ti:C:O:F ratio of a MXene sample from EDS was 35:25:15:25. For both data, Ti/C ratio is close to 3:2, however, the ratio of F/O is different. The surfaces of Ti_3C_2 made in HF solution are always terminated by F and/or OH groups and the ratio of F/OH is variable. Some F and/or OH may be lost during subsequent drying process. Then EDS results are difficult to give us information on the resulted chemistry, especially on F and/or OH groups. Thus, only one EDS result is shown for the purpose of concision.

2D MXene floating in the HF solution after exfoliating were observed by TEM, which are separated by filtering, washed by deionized water, removed to a glass dish and dried in a vacuum oven. The TEM images in Fig. 9 show that MXenes are quite thin and transparent to electrons because other sheets are clearly seen below them. This strongly suggests that these are very thin foils, especially considering the high atomic number of Ti. From SEM results in Fig. 8f and previous TEM result in Ref. [27], we deem that the thickness of a sheet shown in Fig. 9 is ~30 nm. Fig. 9b is a highly magnified image of the area 1 of Fig. 9a. A crystal sheet is shown with an angle of ~120°. Selected area electron diffraction (SAED) pattern of the 2D crystal is shown in the inset of Fig. 9b. It is an obviously hexagonal pattern and matches well with the pattern of Ti_3C_2 MXene reported by previous literature [5,9]. The *d*-spacing estimated from the pattern are 0.252 nm for (1 0 0) planes and 0.182 nm for (1 1 0) planes. There is no PDF card providing *d*-spacing of MXene for comparison. However, these values can be compared with those of Ti_3AlC_2 from PDF card #52-0875, which are 0.266 nm for (1 0 0) planes and 0.153 nm for (1 1 0) planes. Compared with Ti_3AlC_2, Ti_3C_2 keeps the hexagonal structure and *d*-spacing adjusts a little except that the value in *c* direction increases extensively.

3.3. Thermal stability results

Fig. 10 shows the thermogravimetric (TG) curve and differential scanning calorimetric (DSC) curve of MXene (49% HF etching at 60 °C for 24 h) from room temperature (RT) to 1000 °C in argon atmosphere (Fig. 10a) or oxygen atmosphere (Fig. 10b). The resolution of TG measurement and DSC measurement are 0.002 μg and 1 μW, respectively. In Ar atmosphere, the weight change of MXene is divided into three stages. The first stage is 0.38% weight loss from RT to 200 °C. The second stage is 4.48% weight loss from 200 °C to 800 °C. The third stage is 2.47% weight loss from 800 °C to 1000 °C, which is a fast weight loss and corresponds to a broad exothermic peak in DSC curve. The intensity of this peak is 4 mW, which is very weak compared with the strong exothermic peaks in Fig. 10b.

In oxygen atmosphere, TG curve is still divided into three stages. As shown in Fig. 10b, the first stage is 0.54% weight loss from RT to 200 °C. The second stage is 19.63% weight gain from 200 °C to 368 °C and a corresponding sharp and very strong exothermic peak (300 mW) at 285 °C in DSC curve. The third stage is weight loss from 368 °C to 1000 °C and a relatively weak exothermic peak (30 mW) at 386 °C in DSC curve.

Fig. 11 shows the SEM and XRD results of MXene samples after high temperature process at thermal analyzer. Fig. 11a is the SEM micrograph of MXene sample processed at 1000 °C in Ar atmosphere. The sample still kept the loose quasi-2D structure of MXene. Fig. 11b and c is the SEM micrographs of sample processed in O_2 atmosphere at 200 °C or 1000 °C, respectively. From Fig. 11b, at 200 °C, many equiaxial crystals were formed on the surface or edge of 2D structure. A few crystals are large (~1 μm) and most crystals are small (~100 nm). However, the quasi-2D structure of MXene was kept.

From Fig. 11c, at 1000 °C, the crystals grew and connected each other to form a net shape. There was only a little trace of the 2D structure of MXene. Fig. 10d shows the XRD patterns of these samples. In Ar atmosphere, samples after 200 °C process kept the quasi-2D structure of MXene. After 1000 °C process, MXene reacted with O_2 impurity in Ar atmosphere or attached OH groups to form a small quantity of TiO_2, thus weak peaks of rutile (TiO_2) exist in the sample's XRD pattern. In O_2 atmosphere, after 200 °C process, large amount of anatase and small quantity of rutile was formed due to the reaction between MXene with O_2. There is a peak at 23.4° in the XRD patterns for both samples heat treated at 200 °C in Ar or O_2 atmosphere. This peak belongs to $TiOF_2$ [27]. The $TiOF_2$ was formed from the low-temperature reaction between Ti_3C_2 with F termination and the oxygen from atmosphere or O/OH termination. After 1000 °C process, most anatase transformed to rutile and the 23.4° peak of $TiOF_2$ in XRD patterns disappears.

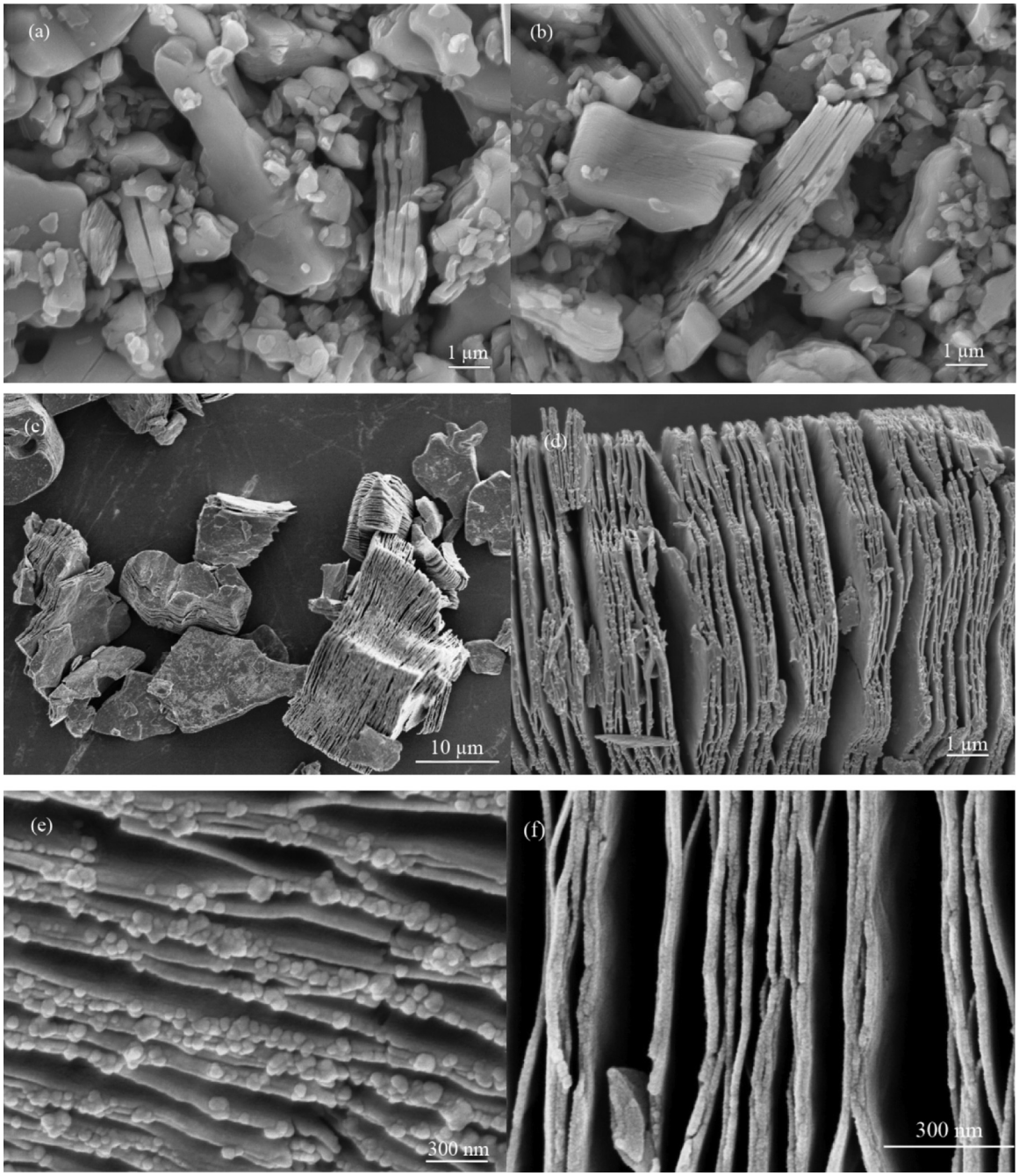

Fig. 8. SEM images of exfoliated Ti_3AlC_2 by 49% HF at 60 °C for (a) 4 h; (b) 8 h; (c) 24 h, low magnification to show all grains are exfoliated; (d) 24 h, high magnification to show a fully exfoliated grain; (e) 24 h, high magnification to show thin layers with small balls with the diameter of 40 ± 10 nm; (f) 24 h, very high magnification to show thin layers without small balls and layer thickness is ~30 ± 5 nm.

4. Discussion

4.1. Exfoliating process to synthesize MXene

From the analysis of aforementioned results (Figs. 3–6), temperature, concentration of HF solution and reaction time are important factors to influence the fabrication of MXene. Different from previous reports [5,6,27] that only 2 h is enough for etching at room temperature, longer time and higher temperature (24 h at 60 °C) were necessary for fully exfoliation of Ti_3AlC_2 to synthesize MXene (Figs. 8 and 9), coinciding within another recently published report [29]. We consider that the discrepancy is caused by the activities of starting material Ti_3AlC_2, which is different as it is obtained by different method. Zhang et al. tried to make a more active Ti_3AlC_2 by synthesizing $Ti_3(Al_xSi_{1-x})C_2$ solid solution [30]. And they exfoliated the $Ti_3(Al_xSi_{1-x})C_2$ solid solution by organic solutions instead of HF. However, the final product they obtained was ultra-thin MAX phase instead of MXene [30]. In this paper, we tried to exfoliate different Ti_3AlC_2 source and explain this discrepancy.

The two kinds of Ti_3AlC_2 have almost same XRD patterns as shown in Fig. 2. However, the XRD patterns in Fig. 6 of MXene powders from the two Ti_3AlC_2 are obviously different. In previous report [6], cold-pressing can significantly enhance the XRD peaks of MXene. However, neither MXene powder from HP-Ti_3AlC_2 nor

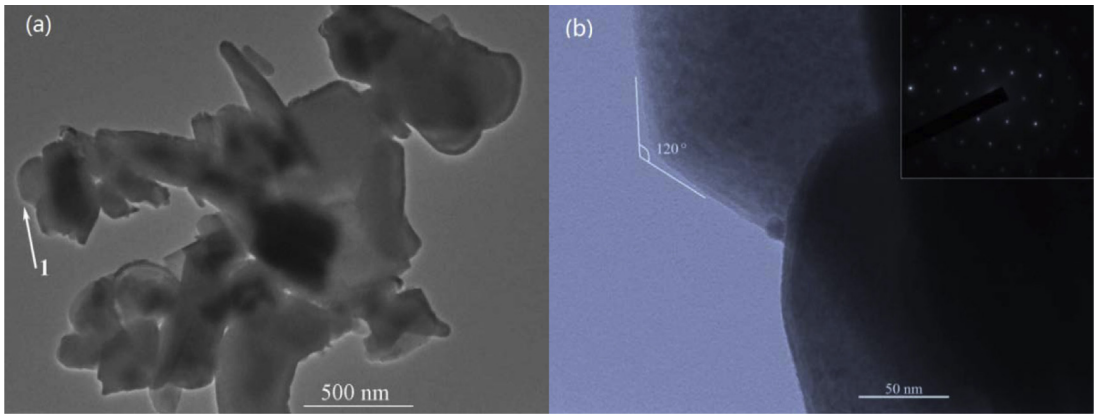

Fig. 9. TEM images of clean Ti_3C_2 2D sheets (a) low magnification, and (b) high magnification. The inset is SAED pattern to show hexagonal structure.

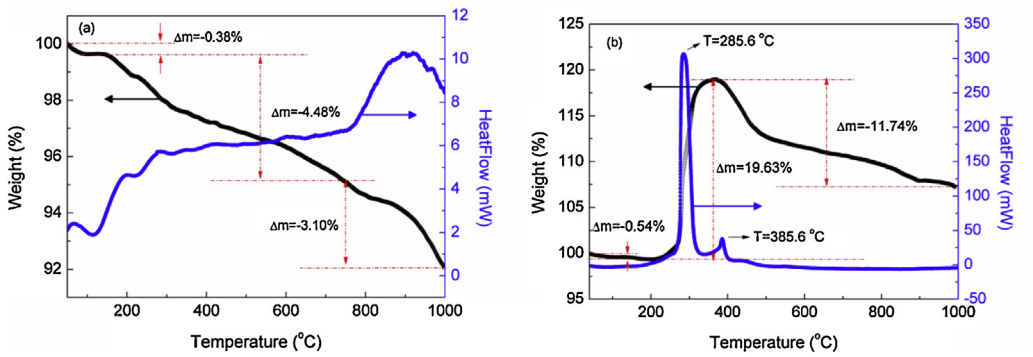

Fig. 10. TG and DSC curves of MXene from room temperature to 1000 °C in (a) argon atmosphere, and (b) oxygen atmosphere.

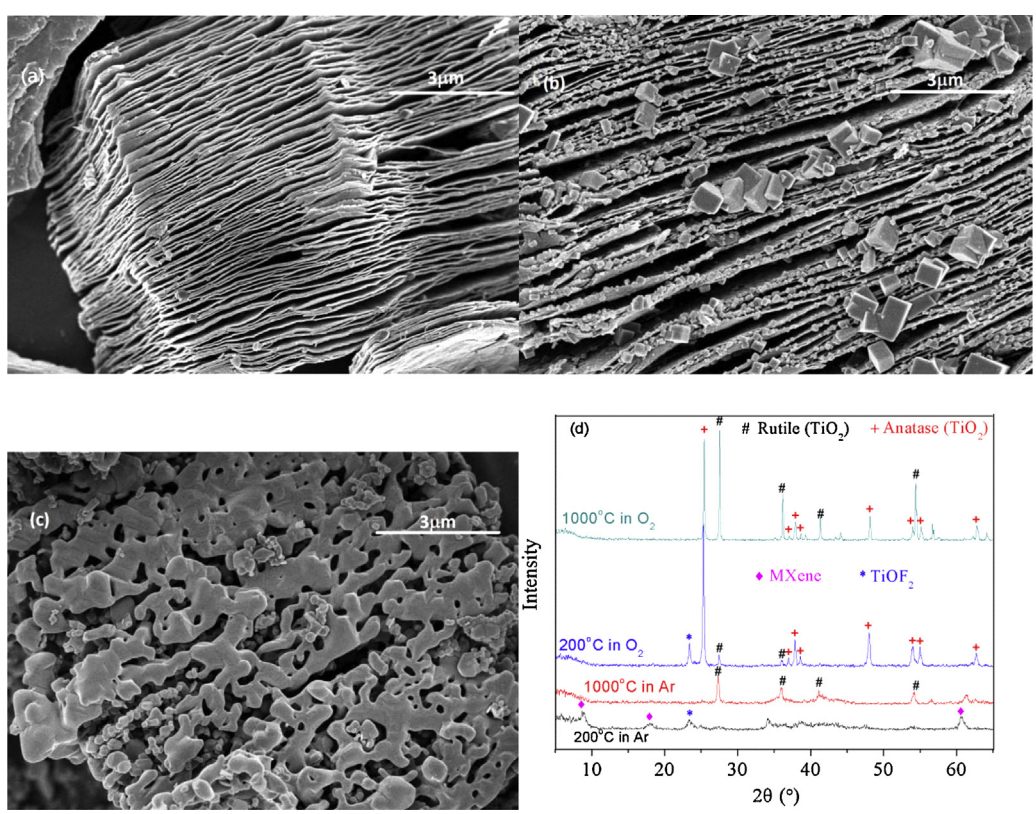

Fig. 11. (a) SEM image of MXene after thermal analysis at 1000 °C in Ar, (b) SEM image of MXene after thermal analysis at 200 °C in O_2, (c) SEM image of MXene after thermal analysis at 1000 °C in O_2, and (d) XRD patterns of MXene after thermal analysis in O_2 or in Ar.

that from PLS-Ti_3AlC_2 was cold pressed for XRD test. Then the difference of XRD patterns is due to starting material rather than the procedure to prepare XRD samples.

The main peaks for TiC impurity is (2 0 0) peak at 41.7° and (1 1 1) peak at 36° degree. Both peaks can be seen in the XRD pattern of Ti_3C_2 from HP-Ti_3AlC_2, but only (1 1 1) peak was observed in case of Ti_3C_2 from PLS-Ti_3AlC_2. This difference is due the preferred orientation of TiC [31]. Besides TiC peaks, Ti_3C_2 peaks also have different relative intensity. Thus, MXene produced from PLS-Ti_3AlC_2 was highly oriented compared to that produced from HP-Ti_3AlC_2. The reason for this difference is not clear at this moment. Consider the lower price of TiH_2, PLS-Ti_3AlC_2 from TiH_2 is a cheaper starting material to synthesize Ti_3C_2 MXene.

From SEM (Fig. 8) and TEM (Fig. 9) images, we observed the fully exfoliated MXene with perfect hexagonal structure. Small balls were found to attach on the edges of MXene as shown in Fig. 8e. It is the first report on this phenomenon. This is important because it solves a mystery in the process to make MXene. The exfoliation of Ti_3AlC_2 follows this equation [5]:

$$Ti_3AlC_2(s) + 3HF(l) \rightarrow Ti_3C_2(s) + AlF_3(s) + (3/2)H_2(g) \quad (1)$$

From Eq. (1), during the etching process, two solid products, Ti_3C_2 crystals and AlF_3, should exist in HF solution. In previous work, however, Ti_3C_2 2D crystal was the only solid that was noticed and researched. AlF_3 cannot dissolve in water, acid and base. The mole ratio of Ti_3C_2:AlF_3 is 1:1. Where is AlF_3? Here were the balls found attached on the edge of MXene sheets. It is very possible that they are AlF_3 that nucleate and grow from HF solution, though we cannot deny the possibility that they are Al's oxide or hydroxide. According to the ratio of Ti_3C_2:AlF_3 in Eq. (1), many AlF_3 balls should be generated. However most of them were washed off or dissolved in HF solution in the form of $AlF_3 \cdot 3H_2O$ during the experiment. Due to the small quantity and small size (40 nm in diameter), it is not detectable to XRD. In our experiment, some balls attached on the edges of 2D sheets were kept and gave us the opportunity to observe them. It is very possible that these balls are AlF_3.

4.2. Intercalation of MXene

From Fig. 7, intercalation with $NH_3 \cdot H_2O$, DMSO, and urea can obviously increase the *LP c* of MXene. This is very helpful to make fully exfoliated MXene 2D sheets. In addition, it is the first report on intercalation of MXene with $NH_3 \cdot H_2O$, which is very cheap compared with other molecules for MXene intercalation.

4.3. Thermal stability of MXene

Ti_3C_2 2D sheets made in HF solution are terminated with F and/or OH [5]. At high temperature, the terminated F and OH are lost or replaced by O. Therefore the amount of terminated F and OH is a key factor to understand the TG and DSC curves. From EDS, Ti:C:F:O atomic ratio of our sample was 28:20:33:18. In previous work [27], the ratio was 35:25:25:15 and a chemical formula was assumed as $Ti_{2.94}C_2F_2O_{0.55}(OH)_{0.65}$. In this paper, based on EDS results and TG/DSC results (Fig. 10), we proposed a simple structure for MXene in this paper: $Ti_3C_2F_2OH$.

As shown in Fig. 10a, in Ar atmosphere, the first stage weight loss (RT to 200 °C) is due to the loss of physically adsorbed water and HF on MXene surface. The second stage weight loss (200–800 °C) is caused by the loss of chemically adsorbed water, which is OH groups attached on Ti_3C_2 surface, as shown by the following equation:

$$Ti_3C_2F_2OH(s) \rightarrow Ti_3C_2F_2O_{0.5}(s) + 0.5H_2O(g) \quad (2)$$

The weight loss calculated from Eq. (2) is 4.05%, which agrees well with the value (4.48%) obtained from TG curve.

At temperature above 800 °C, the obtained $Ti_3C_2F_2O_{0.5}$ starts to lose F or O. Due to different bond energy, the loss of O should be easier than the loss of F. The third stage weight loss in TG curve follows this equation:

$$Ti_3C_2F_2O_{0.5}(s) \rightarrow Ti_3C_2F_2(s) + 0.25O_2(g) \quad (3)$$

The calculated weight loss is 3.59%, approximate to 3.10% measured in TG curve. At higher temperature (>1000 °C, above the limit of our experiment), more O and even F may be lost.

According to this analysis, the heat process of MXene in Ar atmosphere is mainly a weight loss process and there are no obvious chemical reactions, which confirmed by XRD and SEM results in Fig. 11. The weight loss needs energy to desorb water and break the bonds between OH/O/F with Ti_3C_2 crystals. Thus, the corresponding DSC curve should be endothermic. However, as shown in Fig. 10a, the true DSC curve is endothermic only in the first stage, the loss of physically absorbed water. Subsequently, DSC curve completely turns into exothermic, especially in the beginning of second and third stages, which are relevant to the loss of chemically absorbed water. This must be due to the decrease of surface energy. $Ti_3C_2F_2OH$ 2D sheets have very large surface area and high surface energy. They are thermodynamically metastable. As the chemical bonded OH groups are lost as H_2O or O_2, some surface of MXene sheets are changed from Ti—OH to Ti—O or uncoordinated Ti. The newly formed surface is unstable and with high surface energy. In order to decrease surface energy, and due to the attraction between Ti—O on the surface of one sheet and uncoordinated Ti on the surface of another sheet, two sheets are attractive and move closer to form a new metastable structure. As a result, two surfaces transform to a new interface. Some energy is released during the process. This explains the exothermic character of DSC curve in Fig. 10a. However, the exothermic peak is very weak compared with the peaks in Fig. 10b. The heat released is very small. The newly formed interface is very weak. This is proved by the SEM image shown in Fig. 11a. In addition, from Fig. 11d, no new phase was formed except a few TiO_2.

In oxygen atmosphere, the first stage of heat treatment is still a weight loss due to the loss of physically absorbed water and HF. Thereafter, according to XRD results in Fig. 11d, MXene react with O_2 to form TiO_2 in the form of rutile or anatase. However, there are two exothermic peaks in the DSC curve, and two stages (drastic weight gain and slow weight loss) in the corresponding TG curve. Therefore, the oxidation of MXene should be divided into two stages.

The first oxidation stage (second stage in the whole process) is the oxidation of surface layers of MXene to form anatase. This reaction corresponds to the first big exothermic peak in DSC curve and drastic weight gain in TG curve. The newly formed anatase in MXene sheets separates the contact of O_2 with unreacted MXene, which stops the further oxidation of MXene and resists the release of CO_2 formed during the oxidation. As a result, an interesting structure as shown in Fig. 11b is generated that anatase nano-crystals are distributed on conductive MXene 2D sheets. Due to the photocatalytic property of anatase nano-crystals, the structure may have important application in the area of photocatalysis. We already obtained good results in preliminary experiment and will report the results in another paper.

The second oxidation stage (third stage in the whole process) is the oxidation of the residual MXene due to the diffusion of O_2 through newly formed TiO_2 in high temperature, which corresponds to the second exothermic peak in DSC curve (Fig. 10b). As shown by the XRD results in Fig. 11d, high temperature process also results in the transformation of anatase to rutile. Accompanying the formation of TiO_2, CO_2 is also formed and released. The release of CO_2 as well as chemically absorbed OH and F results in the total

weight loss in TG curve. The whole reaction follows this equation:

$$Ti_3C_2F_2OH(s) + 4.75O_2(g) \rightarrow 3TiO_2(s) + 2CO_2(g) + 0.5H_2O(g) + F_2(g) \quad (4)$$

Very recently, Naguib et al. obtained similar results [32]. In their work, flash heating 2D Ti_3C_2 in air resulted in TiO_2 nanocrystals on thin sheets of disordered graphitic carbon and the carbon was burned later in excess of oxygen leaving pure TiO_2 alone. The TG and DSC curves in our paper support the statement in Naguib's paper that TiO_2 and CO_2 were formed from the reaction between Ti_3C_2 and oxygen. However, our experiment was a long time reaction (~20 min for temperature increasing and ~20 min for temperature decreasing), which was different from the flash reaction (the whole reaction time < 5 s) in Naguib's paper [13]. The newly formed carbon was unstable in our experiment. Therefore, we only state that final reaction products were TiO_2, CO_2, F_2 and H_2O as shown in Eq. (4).

Compared with that of corresponding 3D materials, the thermal stability of Ti_3C_2 MXene is worse. Ti_3AlC_2 is stable at least up to 1460 °C in Ar atmosphere [33]. And Ti_3AlC_2 has excellent oxidation resistance in air at the temperature below 1200 °C because continuous α-Al_2O_3 layer is formed to prevent further oxidation [34]. For nanocrystalline titanium carbide with an average diameter of 30 nm, thermal stability and oxidation resistance are good at temperature up to 350 °C in air [35]. Due to high specific surface area, it is not surprising that Ti_3C_2 MXene has worse thermal stability than Ti_3AlC_2 or TiC. However, it is a little surprising that, as a quasi-2D material, Ti_3C_2 MXene has even worse thermal stability, compared with graphene, a typical genuine 2D material with good oxidization resistance at 601 °C in air [36].

5. Conclusions

Ti_3C_2 MXene with quasi-2D structure was successfully prepared. The 2D Ti_3C_2 crystals from Ti_3AlC_2 had perfect hexagonal structure. The influences of temperature, time and the source of Ti_3AlC_2 on the exfoliating process were researched and clarified. Compared with HP-Ti_3AlC_2 from element powders, PLS-Ti_3AlC_2 made by tube furnace from TiH_2 as Ti source is a cheaper starting material to make MXene with highly preferred orientation. A suitable condition to synthesize MXene was achieved in this paper, which is etching for at least 24 h at 60 °C in 49% HF solution. Small balls, which may be AlF_3, as by-products were observed on the edge of MXene sheets. In argon atmosphere, Ti_3C_2 MXene is stable from room temperature to 800 °C. In oxygen atmosphere, at 200 °C, parts of MXene layers are oxidized to an interesting structure: anatase nano-crystals are evenly distributed on 2D Ti_3C_2 sheets. At 1000 °C, MXenes are completely oxidized and rutile is the final oxidized products.

Acknowledgments

This work was supported by National Nature Science Foundation of China (51472075, 51205111), Plan for Scientific Innovation Talent of Henan Province (134100510008), Program for Innovative Research Team of Henan Polytechnic University (T2013-4), State Key Laboratory of New Ceramic and Fine Processing Tsinghua University (KF201313).

References

[1] K.S. Novoselov, A.K. Geim, S.V. Morozov, D. Jiang, Y. Zhang, S.V. Dubonos, I.V. Grigorieva, A.A. Firsov, Science 306 (2004) 666–669.
[2] D. Pacile, J.C. Meyer, Ç.Ö. Girit, A. Zettl, Appl. Phys. Lett. 92 (2008) 133107.
[3] R. Ma, T. Sasaki, Adv. Mater. 22 (2010) 5082–5104.
[4] K.S. Novoselov, D. Jiang, F. Schedin, T.J. Booth, V.V. Khotkevich, S.V. Morozov, A.K. Geim, Proc. Natl. Acad. Sci. U.S.A. 102 (2005) 10451–10453.
[5] M. Naguib, M. Kurtoglu, V. Presser, J. Lu, J. Niu, M. Heon, L. Hultman, Y. Gogotsi, M.W. Barsoum, Adv. Mater. 23 (2011) 4248–4253.
[6] M. Naguib, O. Mashtalir, J. Carle, V. Presser, J. Lu, L. Hultman, Y. Gogotsi, M.W. Barsoum, ACS Nano 6 (2012) 1322–1331.
[7] M. Naguib, J. Come, B. Dyatkin, V. Presser, P.-L. Taberna, P. Simon, M.W. Barsoum, Y. Gogotsi, Electrochem. Commun. 16 (2012) 61–64.
[8] M.R. Lukatskaya, O. Mashtalir, C.E. Ren, Y. Dall'Agnese, P. Rozier, P.L. Taberna, M. Naguib, P. Simon, M.W. Barsoum, Y. Gogotsi, Science 341 (2013) 1502–1505.
[9] D. Sun, M. Wang, Z. Li, G. Fan, L.-Z. Fan, A. Zhou, Electrochem. Commun. 47 (2014) 80–83.
[10] Q. Tang, Z. Zhou, P. Shen, J. Am. Chem. Soc. 134 (2012) 16909–16916.
[11] Q. Hu, D. Sun, Q. Wu, H. Wang, L. Wang, B. Liu, A. Zhou, J. He, J. Phys. Chem. A 117 (2013) 14253–14260.
[12] Q. Peng, J. Guo, Q. Zhang, J. Xiang, B. Liu, A. Zhou, R. Liu, Y. Tian, J. Am. Chem. Soc. 136 (2014) 4113–4116.
[13] Y. Gao, L. Wang, Z. Li, A. Zhou, Q. Hu, X. Cao, Solid State Sci. 35 (2014) 62–65.
[14] I.R. Shein, A.L. Ivanovskii, Comput. Mater. Sci. 65 (2012) 104–114.
[15] G.S. Rohrer, M. Affatigato, M. Backhaus, R.K. Bordia, H.M. Chan, S. Curtarolo, A. Demkov, J.N. Eckstein, K.T. Faber, J.E. Garay, Y. Gogotsi, L. Huang, L.E. Jones, S.V. Kalinin, R.J. Lad, C.G. Levi, J. Levy, J.-P. Maria, L. Mattos, A. Navrotsky, N. Orlovskaya, C. Pantano, J.F. Stebbins, T.S. Sudarshan, T. Tani, K. Scott Weil, J. Am. Ceram. Soc. 95 (2012) 3699–3712.
[16] M. Khazaei, M. Arai, T. Sasaki, C.-Y. Chung, N.S. Venkataramanan, M. Estili, Y. Sakka, Y. Kawazoe, Adv. Funct. Mater. 23 (2013) 2185–2192.
[17] M. Yoshida, Y. Hoshiyama, J. Ommyoji, A. Yamaguchi, Mater. Sci. Eng. B 173 (2010) 126–129.
[18] M.K. Drulis, A. Czopnik, H. Drulis, J.E. Spanier, A. Ganguly, M.W. Barsoum, Mater. Sci. Eng. B 119 (2005) 159–163.
[19] M.W. Barsoum, MAX Phases: Properties of Machinable Ternary Carbides and Nitrides, John Wiley & Sons, 2013.
[20] D. Sun, A. Zhou, Z. Li, L. Wang, J. Adv. Ceram. 2 (2013) 313–317.
[21] M.W. Barsoum, Encyclopedia of Materials: Science and Technology, 2006.
[22] M. Kurtoglu, M. Naguib, Y. Gogotsi, M.W. Barsoum, MRS Commun. 2 (2012) 133–137.
[23] L.-Y. Gan, D. Huang, U. Schwingenschlögl, J. Mater. Chem. A 1 (2013) 13672–13678.
[24] Y. Xie, P. Kent, Phys. Rev. B 87 (2013) 235441.
[25] A.N. Enyashin, A.L. Ivanovskii, J. Solid State Chem. 207 (2013) 42–48.
[26] L. Li, A. Zhou, L. Xu, Z. Li, L. Wang, J. Wuhan Univ. Technol.-Mater. Sci. Ed. 28 (2013) 882–887.
[27] O. Mashtalir, M. Naguib, B. Dyatkin, Y. Gogotsi, M.W. Barsoum, Mater. Chem. Phys. 139 (2013) 147–152.
[28] O. Mashtalir, M. Naguib, V.N. Mochalin, Y. Dall'Agnese, M. Heon, M.W. Barsoum, Y. Gogotsi, Nat. Commun. 4 (2013) 1716.
[29] F. Chang, C. Li, J. Yang, H. Tang, M. Xue, Mater. Lett. 109 (2013) 295–298.
[30] X. Zhang, J. Xu, H. Wang, J. Zhang, H. Yan, B. Pan, J. Zhou, Y. Xie, Angew. Chem. Int. Ed. 52 (2013) 4361–4365.
[31] L.-Y. Kuo, P. Shen, Mater. Sci. Eng. A 276 (2000) 99–107.
[32] M. Naguib, O. Mashtalir, M.R. Lukatskaya, B. Dyatkin, C. Zhang, V. Presser, Y. Gogotsi, M.W. Barsoum, Chem. Commun. 50 (2014) 7387–7554.
[33] X.H. Wang, Y.C. Zhou, Chem. Mater. 15 (2003) 3716–3720.
[34] X.H. Wang, Y.C. Zhou, Corros. Sci. 45 (2003) 891–907.
[35] J. Ma, M. Wu, Y. Du, S. Chen, G. Li, J. Hu, Mater. Sci. Eng. B 153 (2008) 96–99.
[36] Z.-S. Wu, W. Ren, L. Gao, J. Zhao, Z. Chen, B. Liu, D. Tang, B. Yu, C. Jiang, H.-M. Cheng, ACS Nano 3 (2009) 411–417.